

July 2013

AN ADVANCED CURRENT CONTROLLER TECHNIQUE BASED ACTIVE POWER FILTER FOR POWER QUALITY IMPROVEMENT

MRS. DIPTI A. TAMBOLI

SVERI'S College of Engineering, Pandharpur, Maharashtra, India 413304., dipti_tamboli@rediffmail.com

D. R. PATIL

Walchand College of Engineering, Maharashtra, India 416415., dadasorpatil@gmail.com

Follow this and additional works at: <https://www.interscience.in/ijpsoem>



Part of the [Power and Energy Commons](#)

Recommended Citation

TAMBOLI, MRS. DIPTI A. and PATIL, D. R. (2013) "AN ADVANCED CURRENT CONTROLLER TECHNIQUE BASED ACTIVE POWER FILTER FOR POWER QUALITY IMPROVEMENT," *International Journal of Power System Operation and Energy Management*. Vol. 2 : Iss. 3 , Article 11.

Available at: <https://www.interscience.in/ijpsoem/vol2/iss3/11>

This Article is brought to you for free and open access by Interscience Research Network. It has been accepted for inclusion in International Journal of Power System Operation and Energy Management by an authorized editor of Interscience Research Network. For more information, please contact sritampatnaik@gmail.com.

AN ADVANCED CURRENT CONTROLLER TECHNIQUE BASED ACTIVE POWER FILTER FOR POWER QUALITY IMPROVEMENT

MRS. DIPTI A. TAMBOLI¹ & D. R. PATIL²

¹SVERI'S College of Engineering, Pandharpur, Maharashtra, India 413304.

²Walchand College of Engineering, Maharashtra, India 416415.

E-mail: dipti_tamboli@rediffmail.com, dadasorpatil@gmail.com

Abstract- Power Quality issues are becoming a major concern for today's power system engineers. Large scale incorporation of non-linear loads has the potential to raise harmonic voltages and currents in an electrical distribution system to unacceptable high levels that can adversely affect the system. Active power filter (APF) based on power electronic technology is currently considered as the most competitive equipment for mitigation of harmonics and reactive power simultaneously. Instantaneous power theory is used for generation of reference current. This paper presents a comparative study of the performance of three current control strategies namely ramp comparison method, hysteresis current controller (HCC) and Adaptive hysteresis current controller (AHCC) and superiority of AHCC is established. Simulation results for all the methods are presented using MATLAB/SIMULINK power system toolbox demonstrating the effectiveness of using adaptive hysteresis band.

Keywords- Active power filter, Harmonics, Instantaneous power theory, hysteresis current control, AHCC

I. INTRODUCTION

SOLID-STATE control of ac power using thyristors and other semiconductor switches is widely employed to feed controlled electric power to electrical loads, such as adjustable speed drives (ASD's), furnaces, computer power supplies, as well as in HVDC systems. Since, being non linear loads, these solid-state converters draw harmonic and reactive power components of current from ac mains. These injected harmonics, reactive power burden, unbalance, and excessive neutral currents cause low system efficiency and poor power factor. They also cause disturbance to other consumers and interference in nearby communication networks. Extensive surveys [1, 2] have been carried out to quantify the problems associated with electric power networks having nonlinear loads. Conventionally passive L-C filters have limitations of fixed compensation, large size, and resonance. The increased severity of harmonic pollution in power networks has attracted the attention of power electronics and power system engineers to develop dynamic and adjustable solutions to the power quality problems [3]. Such equipment is generally known as active power filters (APF's).

Shunt active filters theories and applications have become more and more popular and have attracted much attention. APF's adopt intelligent circuits to measure harmonic and reactive power of nonlinear loads and take corrective actions. By injecting compensation current with 180° phase shift with load current at the point of common coupling where the nonlinear load is connected, the sinusoidal source currents are maintained. Therefore, both harmonic suppression and reactive power compensation for the nonlinear load are achieved.

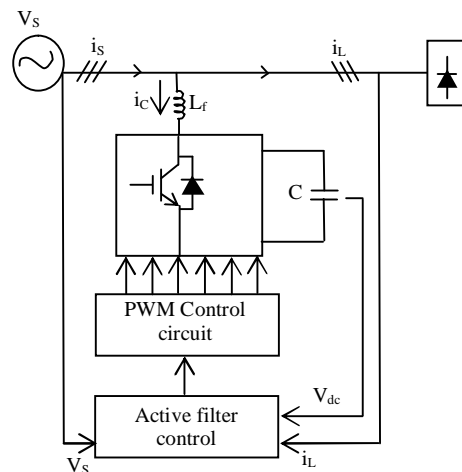


Fig 1. APF control block

One of the peculiar features of shunt APFs is that it does not require energy storage units such as batteries or active sources in other forms for its compensation mechanism. To accomplish this function, it requires an effective reference compensation strategy for both reactive and harmonic power of the load. Generally, the performance of APF is based on three design criteria [4-12]: (i) design of power inverter; (ii) types of current controllers used; (iii) methods used to obtain the reference current. Many control techniques have been used to obtain the reference current [6-12]. Among these controllers the instantaneous real-power theory provides good compensation characteristics in steady state as well as transient states [4-5]. Fig. 1 shows a system control block for a three-phase shunt APF.

Similarly various current controller techniques proposed for APF configuration, such as triangular-current controller, periodical-sampling controller and

hysteresis current controller. In ramp comparison method multiple crossings of the ramp by the current error may become a problem when the time rate change of the current error becomes greater than that of the ramp. Therefore nowadays, hysteresis current controller method attracts researcher’s attention due to unconditional stability, fast transient response, simple implementation and high accuracy. However, this control scheme exhibits several unsatisfactory features such as uneven switching frequency and switching frequency variation within a particular band. The adaptive-hysteresis current controller overcomes these demerits of HCC; adaptive- HCC changes the bandwidth according to instantaneous compensation current variation. This paper presents design and analysis of an active power filter that uses instantaneous power-theory with three types of current controller which generates switching pulses for APF. The shunt APF is investigated under non-linear load and found to be effective for harmonics and reactive power compensation according to IEEE standards.

The simulation is carried out using MATLAB/Simulink for two different types of non-linear loads and at different firing angles. This entire simulation studies were carried out by choosing an 11Kv feeder providing supply to Walchand College of Engineering, Sangli, India.

II. INSTANTANEOUS REACTIVE POWER THEORY (P-Q THEORY)

In 3-phase circuits with balanced voltage, instantaneous currents and voltages are converted into instantaneous space

Vectors [13, 14]. The traditional definitions of the power components are all based on the direct quantities of 3-phase voltages and currents vectors: e_a, e_b, e_c and i_a, i_b, i_c . In instantaneous reactive power theory, the instantaneous 3-phase currents and voltages are expressed as the following equations. These space vectors are easily converted into α - β coordinates.

$$\begin{bmatrix} e_\alpha \\ e_\beta \end{bmatrix} = \sqrt{2/3} \begin{bmatrix} 1 & 1/2 & 1/2 \\ 0 & \sqrt{3}/2 & -\sqrt{3}/2 \end{bmatrix} \begin{bmatrix} e_a \\ e_b \\ e_c \end{bmatrix} \tag{1}$$

$$\begin{bmatrix} i_\alpha \\ i_\beta \end{bmatrix} = \sqrt{2/3} \begin{bmatrix} 1 & -1/2 & -1/2 \\ 0 & \sqrt{3}/2 & -\sqrt{3}/2 \end{bmatrix} \begin{bmatrix} i_a \\ i_b \\ i_c \end{bmatrix} \tag{2}$$

And α, β are orthogonal coordinates. e_α and i_α are on α axis, e_β and i_β are on β axis. When the source supplies nonlinear loads, the instantaneous power delivered to the loads includes both active and reactive components. So, the current vector i was divided into active current component and reactive

current component, which are i_p and i_q respectively, as shown in Fig.2

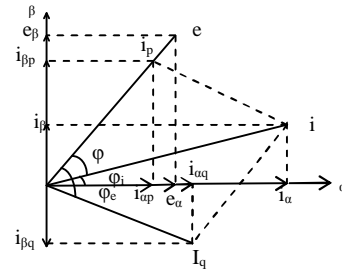


Fig.2 Vector diagram of voltage and currents

In the representation of electric quantities, instantaneous active and reactive powers are calculated as follows:

$$P = e \cdot i_p, \quad q = e \cdot i_q,$$

Where, $i_p = I \cos\phi, i_q = I \sin\phi$ make up Eq. (3):

$$\begin{bmatrix} \bar{p} \\ \tilde{q} \end{bmatrix} = \begin{bmatrix} \bar{p} + \tilde{p} \\ \tilde{q} + \tilde{q} \end{bmatrix} = \begin{bmatrix} e_\alpha & e_\beta \\ -e_\beta & e_\alpha \end{bmatrix} \begin{bmatrix} i_\alpha \\ i_\beta \end{bmatrix} \tag{3}$$

Here, “—” and “~” stand for dc and ac components, respectively. \bar{p} and \tilde{q} are the instantaneous active and reactive power (dc value) originating from the symmetrical fundamental (positive-sequence) component of the load current, \tilde{p} and \tilde{q} are the instantaneous active and reactive power (ac value) originating from harmonic and the asymmetrical fundamental (negative-sequence) component of the load current. These power quantities given above for an electrical system are represented in a-b-c coordinates and have the following physical meaning:

\bar{p} =The mean value of the instantaneous active power—corresponds to the energy per time unit transferred from the power supply to the load, through a-b-c coordinates, in a balanced way.

\tilde{p} =Alternated value of the instantaneous active power it is the energy per time unit that is exchanged between the power supply and the load through a-b-c coordinates.

\bar{q} =Instantaneous reactive power—corresponds to the power that is exchanged between the phases of the load. This component does not imply any exchange of energy between the power supply and the load, but is responsible for the existence of undesirable currents, which circulate between the system phases.

\tilde{q} =The mean value of the instantaneous reactive power that is equal to the conventional reactive power.

From Eq.(3), in order to measure the harmonic currents and reactive current component, fundamental

active current corresponding to reactive power on α - β coordinates should be first calculated by Eq.(4):

$$\begin{bmatrix} i_{\alpha f} \\ i_{\beta f} \end{bmatrix} = C_{\beta\alpha}^{-1} \begin{bmatrix} \bar{p} + p_{loss} \\ 0 \end{bmatrix} \quad (4)$$

The fundamental active currents in α - β reference frame are then transformed into a-b-c reference frame and they are:

$$\begin{bmatrix} i_{\alpha f} \\ i_{\beta f} \\ i_{\gamma f} \end{bmatrix} = \sqrt{2/3} \begin{bmatrix} 1 & 0 \\ -1/2 & \sqrt{3/2} \\ -1/2 & -\sqrt{3/2} \end{bmatrix} \begin{bmatrix} i_{\alpha f} \\ i_{\beta f} \end{bmatrix} \quad (5)$$

Finally, the reference compensation currents are obtained by Eq. (6):

$$\begin{bmatrix} i_{\alpha}^* \\ i_{\beta}^* \\ i_{\gamma}^* \end{bmatrix} = \begin{bmatrix} i_{L\alpha} \\ i_{L\beta} \\ i_{L\gamma} \end{bmatrix} - \begin{bmatrix} i_{\alpha f} \\ i_{\beta f} \\ i_{\gamma f} \end{bmatrix} \quad (6)$$

The DC side voltage of APF should be controlled and kept at a constant value to maintain the normal operation of the inverter. Because there is energy loss due to conduction and switching power losses associated with the diodes and IGBTs of the inverter in APF, which tend to reduce the value of V_{dc} across capacitor C_{dc} . A feedback voltage control circuit needs to be incorporated into the inverter for this reason. The difference between the reference value, V_{ref} and the feedback value (V_{dc}), an error function first passes a PI regulator and the output of the PI regulator is added in the alpha axis value of the fundamental current components.

III. CURRENT CONTROLLER TECHNIQUE

A. Ramp comparison controller

The controller can be thought of as producing sine-triangle PWM with the current error considered to be the modulating function. The current error is compared to a triangle waveform and if the current error is greater(less) than the triangle waveform, and then the inverter leg is switched in the positive (negative) direction. With sine-triangle PWM, the inverter switches at the frequency of the triangle wave and produces well defined harmonics. Multiple crossings of the ramp by the current error may become a problem when the time rate change of the current error becomes greater than that of the ramp. However, such problems can be adjusted by changing the amplitude of the triangle wave suitably.

B. Hysteresis controller [15]

The hysteresis band current control can be implemented to generate the switching pattern in order to get precise and quick response. The hysteresis band current control technique has proven to be most suitable for all the applications of current controlled voltage source inverters in active power

filters. The hysteresis band current control is characterized by unconditioned stability, very fast response, good accuracy, and inherent-peak current limiting capability, the technique does not need any information about system parameters.

The conventional hysteresis band current control scheme used for the control of active power filter line current is shown in Fig.3, composed of a hysteresis around the reference line current [15].

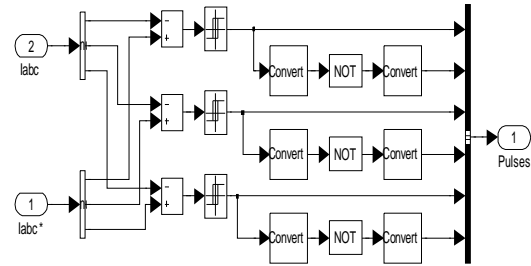


Fig.3 Simulation diagram of hysteresis current controller

The reference line current of the active power filter is referred to as I_{ca}^* , and actual line current of the active power filter is referred to as I_{ca} . The hysteresis band current controller decides the switching pattern of active power filter. The switching logic is formulated as follows: If $i_{ca} < (I_{ca}^* - HB)$ upper switch is OFF and lower switch is ON for leg “a” : (SA=1). If $i_{ca} > (I_{ca}^* + HB)$ upper switch is ON and lower switch is OFF for leg “a” (SA=0). The switching functions SB and SC for phases B and C are determined similarly, using corresponding reference and measured currents and hysteresis bandwidth (HB). The switching frequency of the hysteresis band current control method described above depends on how fast the current changes from the upper limit of the hysteresis band to the lower limit of the hysteresis band, or vice versa.

C. Adaptive hysteresis current controller

Width of the hysteresis band determines the allowable current shaping error to control the switching frequency of the inverter. As the bandwidth narrows the switching frequency increases. A suitable bandwidth should be selected in accordance with the switching capability of the inverter. The bandwidth should also be small enough to supply the reference current precisely keeping the view of switching losses and EMI related problems. Therefore, the range of switching frequencies used is based on a compromise between these factors. By changing the bandwidth, which changes the average switching frequency of the APF, user can evaluate the performance for different value of hysteresis bandwidth. Switching frequency of the hysteresis band current controller is depends on the rate of change of the actual APF current and therefore switching frequency varies along with the current waveform. Line inductance of the APF and the dc bus voltage are the main parameters determining the rate of change of the

actual APF currents. Therefore switching frequency also depends on these two parameters.

Fig. 4 shows the PWM current and voltage waves for phase a [16]. When the actual line current of the active power filter tries to leave the hysteresis band, the suitable IGBT is switched to ON or OFF to force the current to return to a value within the hysteresis band. Then the switching pattern will be trying to maintain the current inside the hysteresis band. Current i_{ca} tends to cross the lower hysteresis band at point 1, where upper side IGBT of leg 'a' is switched on. The linearly rising current i_{ca}^+ then touches the upper band at point 2, where the lower side IGBT of leg 'a' is switched on. The following equations can be written in the respective switching intervals t_1 and t_2 .

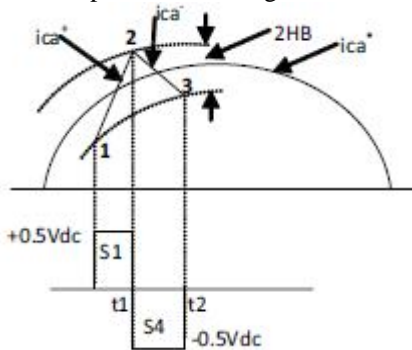


Fig.4 Current and Voltage waves with AHCC

$$L \frac{di_{ca}^+}{dt} = (0.5 V_{dc} - V_f) \quad (7)$$

$$L \frac{di_{ca}^-}{dt} = -(0.5 V_{dc} + V_f) \quad (8)$$

$$\frac{di_{ca}^+}{dt} + \frac{di_{ca}^-}{dt} = 0 \quad (9)$$

where L is phase inductance, and i_{ca}^+ and i_{ca}^- are the respective rising and falling current segments. From the geometry of Fig. 4, we can write

$$\frac{di_{ca}^+}{dt} t_1 + \frac{di_{ca}^-}{dt} t_1 = 2 * HB \quad (10)$$

$$\frac{di_{ca}^-}{dt} t_2 - \frac{di_{ca}^+}{dt} t_2 = -2 * HB \quad (11)$$

$$t_1 + t_2 = T_c = \frac{1}{f_c} \quad (12)$$

where t_1 and t_2 are the switching intervals, and f_c is the switching frequency.

Adding (10) and (11) and substituting in (12), we get

$$t_1 \frac{di_{ca}^+}{dt} + t_2 \frac{di_{ca}^-}{dt} - \frac{1}{f_c} \frac{di_{ca}^+}{dt} = 0 \quad (13)$$

Subtracting (11) from (10), we get

$$4HB = \frac{di_{ca}^+}{dt} t_1 - \frac{di_{ca}^-}{dt} t_2 - (t_1 - t_2) \frac{di_{ca}^+}{dt} \quad (14)$$

Substituting (9) in (13) and (14) and simplifying

$$4HB = (t_1 + t_2) \frac{di_{ca}^+}{dt} - (t_1 - t_2) \frac{di_{ca}^-}{dt} = 0 \quad (15)$$

$$(t_1 - t_2) = \left(\frac{di_{ca}^+}{dt} \right) / f_c \left(\frac{di_{ca}^+}{dt} \right) \quad (16)$$

Substituting (16) in (15), gives

$$HB = \left\{ \frac{0.433V_{dc}}{f_c L} \left[1 - \frac{4z^2}{V_{dc}^2} \left(\frac{V_f}{L} + m \right)^2 \right] \right\} \quad (17)$$

where m is the slope of command current wave. Hysteresis band (HB) can be modulated at different points of fundamental frequency to control the switching patterns of the inverter. For symmetrical operation of all three phases, it is expected that the hysteresis band width (HB) profiles HBa, HBb and HBc will be the same, but have phase difference. The variable HCC is used to produce gate control pulses that operate the voltage source inverter.

IV. SIMULATION RESULT

A typical distribution feeder originating from a substation to Walchand College of Engineering, Sangli campus load centers has been considered for simulation. A three-phase 11Kv/433V, Dy11 transformer is employed in the Institute for catering to the loads locally. Walchand College of Engineering, Sangli is getting supply from MSEDL through 11 KV feeder which is modeled and referred to low voltage side. Therefore the values for source impedance come out to be 0.02871 Ω , 0.2047 mH. Source voltage is considered as 440 v and of 50 Hz frequency. Filter parameters are selected as $L_f = 4$ mH, $V_{dc} = 850$ V, $C_{dc} = 1400$ μ F.

The performances of ramp comparison method, HCC and AHCC based shunt active power filter were evaluated through simulation using MATLAB/SIMULINK environment. A thyristor converter with R-L load is taken as $t=0$ to $t=0.1$ with resistance of 100 Ω and inductance of 50 mH under steady state and for remaining transient period R-L with 50 Ω and inductance of 25 mH.

The simulation results in transient operation using AHCC are presented in Fig. 5 The Waveform of the source current without APF and its THD are shown in Fig.5 (a) and (b) respectively. These current waveforms are for a particular phase (phase a). Other phases are not shown as they are only phase shifted by 120° and we have considered only a balanced load. Also the Waveform of the source current with APF and its THD are shown in Fig.5(c) and (d) respectively. The APF supplies the compensating current to PCC, which is shown in Fig. 5(e). The time domain response of the p-q theory controller is shown in Fig. 5(f) which clearly indicates that, the controller

output settles after a few cycles. The capacitor voltage superimposed to its reference is shown in Fig. 5(f). In order evaluate the good performance of the control, the total harmonic distortion (THD) is measured for the source current before and after compensation. It shows that THD improves from 27.78% to 1.49 % using Adaptive hysteresis current controller with the APF.

The system is simulated at different operating conditions such as thyristor convertor with firing angle of 0° and 30° . The final values of THD of source current before and after compensation as well as capacitor voltage after compensation are listed in Table I. The source current is giving better result using AHCC than other controllers and their THD's are below the specifications prescribed by IEEE 519 standard recommendations on harmonics levels.

Table I
Source Current Total Harmonic Distortion: Thd%

Type of current controller	Load THD%			Source THD%			PQ before	PQ after	Vdc
$\alpha=0^{\circ}$									
SPWM	25.79	25.8	25.79	1.6	1.6	1.61	10.22 KW, 1.56 KVAR	10.27 KW, 4.97 VAR	855.3
HCC (h=0.9)	25.76	25.76	25.76	1.57	1.59	1.64	10.23 KW, 1.55 KVAR	10.27 KW, 7.1 VAR	851.3
AHCC	25.78	25.78	25.78	1.49	1.51	1.48	10.22 KW, 1.55 KVAR	10.27 KW, 1.29 VAR	851.6
$\alpha=30^{\circ}$									
SPWM	29.99	30.02	30.01	2.92	2.95	2.96	8.51 KW, 4.01 KVAR	8.54 KW, 7.9 VAR	856.7
HCC (h=0.9)	30.00	30.02	30.01	2.71	2.86	2.84	8.504 KW, 4.00 KVAR	8.54 KW, 9.33 VAR	852.3
AHCC	30.00	30.03	30.01	2.79	2.83	2.77	8.5 KW, 4.00 KVAR	8.54 KW, 3.4 VAR	853.2

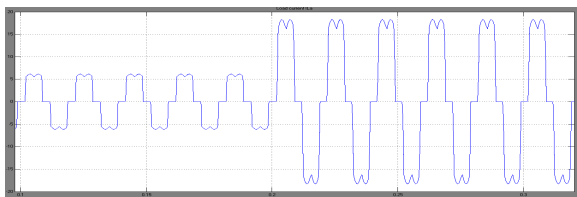


Fig.5.a.Source current without APF

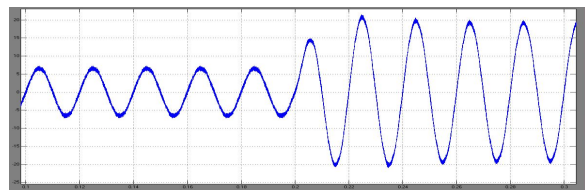


Fig.5.c.Source current with APF

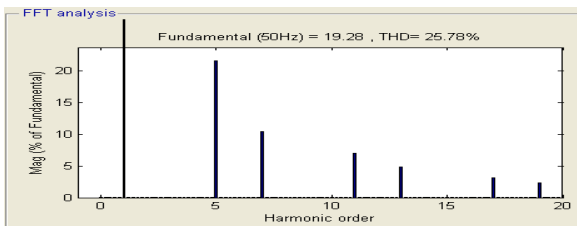


Fig.5.b.THd of source current without APF

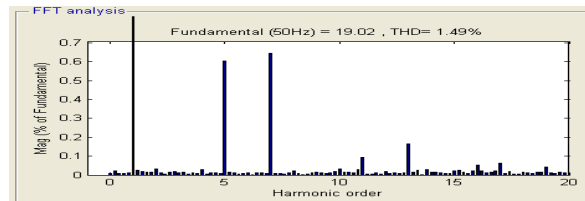


Fig.5.d.THd of source current with APF

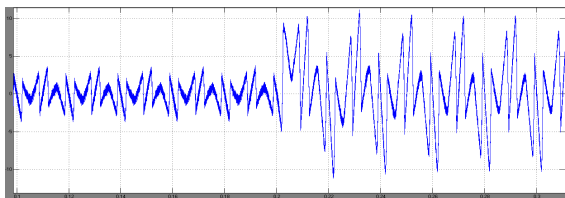


Fig.5.e.Compensating current

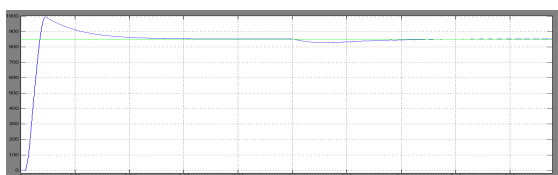


Fig.5.f. Capacitor voltage superimposed to its reference

V. CONCLUSION

An AHCC has been implemented for three phase shunt active power filter. The instantaneous power theory is used to extract the reference currents from the distorted line currents. This facilitates enhancement of power quality through reactive power compensation and harmonics suppression due to nonlinear load. The results obtained indicate that DC-capacitor voltage and the harmonic current can be controlled easily for various load conditions. The performance of the AHCC, fixed HCC and ramp controller technique shunt active power filter are verified and compared with the simulation results. The

THD of the source current after compensation is 1.49% which is less than 5%, the harmonic limit

imposed by the IEEE-519 standard.

REFERENCES

- [1] H. Akagi, "New Trends in Active Filters for power conditioning", IEEE Tran. On Industry applications, Vol 32, No 6, Nov./Dec. 1996.
- [2] A book on "Uninterruptible power supplies and Active filters", Ali Emadi, Abdolhosein Nasiri and S. Bekiarov, CRC Press.
- [3] H. Akagi, "Modern active filters and traditional passive filters," Bulletin of the polish academy of science, Vol. 54, No. 3, 2006.
- [4] Z. Peng, H. Akagi and A. Nabae, "A Novel Harmonic Power Filter," IEEE Power Electronics Specialists Conference RECORD, pp. 1151-1159, 1988.
- [5] H. Akagi, Y. Kanazawa and A. Nabae, "Instantaneous Reactive Power Compensators Comprising Switching Devices without Energy Storage Components," IEEE Transactions on Industry Applications, Vol. IA-20, No. 3, pp. 625-630, 1984.
- [6] Bhattacharya S., Divan, and B. Benezee, "Synchronous Reference Frame Harmonic Isolator Using Series Active Filter", 4th European Power Electronic Conf., Florence, Vol. 3, (1991);pp. 30-35.
- [7] Saetio S, Devaraj R, Tomey D. The design and implementation of a three phase active power filter based on sliding mode control. IEEE T Ind Appl 1995; 31:993_1000.
- [8] Singh B, Al-Haddad K, Chandra A. Active power filter with sliding mode control. In: Proc Inst Elect Eng, Generation Transm Distrib; 1997, vol. 144. p. 564_8.
- [9] Rastogi M, Mohan N, Edris A. Hybrid-active power filtering of harmonic currents in power systems. IEEE T Power Del 1995; 10(3): 1994_2000.
- [10] Bhattacharya S, Veliman A, Divan A, Lorenz R. Flux based active power filter controller. In: Proc IEEE-IAS Annual Meeting Record; 1995. p. 2483_91.
- [11] Jou H. Performance comparison of the three-phase active power filters algorithms. In: Proc. Inst. Elect. Eng., Generation Transm. Distrib; 1995, vol. 142. p. 646_52.
- [12] Dixon J, Garcia J, Moran I. Control system for three-phase active power filters which simultaneously compensates power factor and unbalanced loads. IEEE T Ind Electron 1995; 42(6):636_41.
- [13] "Simulation and reliability analysis of shunt active power filter based on instantaneous reactive power theory", CUI Yu-long1, LIU Hong, WANG Jing-qin, SUN Shu-guang, Journal of Zhejiang University SCIENCE an ISSN ,2007.
- [14] H. Akagi, A. Nabae and S. Atoh, "Control Strategy of Active Power Filters Using Multiple Voltage Source PWM Converters," IEEE Transactions on Industry Applications, Vol. IA-22, No. 3, pp. 460- 465, 1986.
- [15] Kale M. and Ozdemir E. "A Novel Adaptive Hysteresis Band Current Controller for Shunt Active Power Filter" IEEE 2003.
- [16] Bose B.K., "An Adaptive Hysteresis Band Current Control Technique of a Voltage Feed PWM Inverter for Machine Drive System," IEEE Transaction on Industrial Electronics, vol.37 no:5 , pp.402-406, October 1990.

Mrs. Dipti Amol Tamboli was born in Maharashtra, India, in 1979. She received the B.E. degree in electrical engineering and the M. Tech. degree in Control systems from Walchand College of Engineering, Sangli, Maharashtra, India, in 2000 and 2012, respectively. Her research interests include the application of power electronics in power systems, electric drives and ANN.



Dr. D. R. Patil aged 53 has obtained his B.E. (Electrical) Degree in First Class in 1983 and M.E. (Electrical) Degree in First Class from Shivaji University, Kolhapur (MS). He also obtained the Ph.D. Degree from the same university in 2012. He started his teaching carrier from 1985, as a Lecturer in Electrical Department of Walchand College of Engineering, Sangli (MS). Subsequently in 1993 he was promoted to Assistant Professor of Control Systems on the Post Graduate. He has about 15 International Conference and 10 National Conference / Seminars publications. He was a Chairman, Board of Studies; Member of Academic Council of Shivaji University, Kolhapur during 2001-2005. His areas of interest are Control Systems and power systems.

